

DiRW: Path-Aware Digraph Learning for Heterophily

Daohan Su, Xunkai Li, Zhenjun Li, Yinping Liao, Rong-Hua Li, Guoren Wang

ABSTRACT

Recently, graph neural network (GNN) has emerged as a powerful representation learning tool for graph-structured data. However, most approaches are tailored for undirected graphs, neglecting the abundant information embedded in the edges of directed graphs (digraphs). In fact, digraphs are widely applied in the real world (e.g., social networks and recommendations) and are also confirmed to offer a new perspective for addressing topological heterophily challenges (i.e., connected nodes have complex patterns of feature distribution or labels). Despite recent significant advancements in DiGNNs, existing spatial- and spectral-based methods have inherent limitations due to the complex learning mechanisms and reliance on high-quality topology, leading to low efficiency and unstable performance. To address these issues, we propose Directed Random Walk (DiRW), which can be viewed as a plug-and-play strategy or an innovative neural architecture that provides a guidance or new learning paradigm for most spatial-based methods or digraphs. Specifically, DiRW incorporates a direction-aware path sampler optimized from the perspectives of walk probability, length, and number in a weight-free manner by considering node profiles and topological structure. Building upon this, DiRW utilizes a node-wise learnable path aggregator for generalized messages obtained by our proposed adaptive walkers to represent the current node. Extensive experiments on 9 datasets demonstrate that DiRW: (1) enhances most spatial-based methods as a plug-and-play strategy; (2) achieves SOTA performance as a new digraph learning paradigm.

KEYWORDS

Graph Neural Network; Directed Graphs; Random Walk

ACM Reference Format:

Daohan Su, Xunkai Li, Zhenjun Li, Yinping Liao, Rong-Hua Li, Guoren Wang. 2024. DiRW: Path-Aware Digraph Learning for Heterophily. In *Proceedings of ACM Conference (Conference'17)*. ACM, New York, NY, USA, 14 pages. <https://doi.org/10.1145/nnnnnnnn.nnnnnnnn>

1 INTRODUCTION

Graph neural networks (GNNs) have been widely used across node- [23, 47, 50], link- [22, 42, 57], and graph-level tasks [24, 27, 43] and achieve satisfactory performance. Therefore, this graph-based deep learning technique holds great potential for applications, such as recommendation [7, 39, 54], financial analysis [4, 16, 35], and

healthcare [2, 33]. Despite their effectiveness, existing methods often overlook edge direction in natural graphs, leading to inevitable information loss and limited performance upper bound.

Compared to undirected representation, digraphs are crucial for modeling the complex topologies present in the real world (e.g., web flow monitoring and bioinformatics), capturing more intricate node relationships. Additionally, the recently proposed A2DUG [29], Dir-GNN [36] and ADPA [40] reveal a key insight: *Edge direction offers a new perspective for effectively addressing the topological heterophily challenges that plague graph learning*. Despite the growing attention towards DiGNNs, this field is still in its infancy and faces the following inherent limitations. (1) Spatial-based methods often stack multiple convolution layers and employ two independent sets of learnable parameters to capture directed information concealed in the out-edges and in-edges, resulting in over-smoothing concerns [53] and high computational costs [13, 19, 61]. (2) Spectral-based methods heavily rely on high-quality directed topology [44, 59], and without this, extreme eigenvalues inevitably lead to sub-optimal performance. Meanwhile, strict theoretical assumptions affect practicality, which hinders their effective deployment in complex real-world scenarios. Therefore, it is urgent to develop a more efficient paradigm for digraph learning.

To enhance the usability of DiGNNs, this paper focuses on spatial-based methods and proposes a novel (directed) path-based learning mechanism (Di)PathGNNs. As we all know, the entanglement of homophily and heterophily, where connected nodes exhibit intricate feature distributions and labels, has recently posed a significant challenge [26, 28, 34, 60]. Researchers strive to achieve robust learning within this complex topology. In this context, compared to the traditional message passing (i.e., neighbor expansion with strict spatial symmetry that disregards edge direction), we highlight the following advantages of DiRW to further clarify the motivation of our study: (1) **Edge Direction and Node Order**. The core of DiPathGNNs lies in performing well-designed random walks for each node, treating the paths as node-wise sequences. *Advantage: DiRW fully considers edge direction and preserves the order of nodes within the walking paths, which is crucial for capturing structural insights.* (2) **Adaptive Expansion of Node Receptive Fields**. DiPathGNNs adaptively extend hop-based neighbors to path-based neighbors by considering the characteristics of random walk, incorporating more homophilous signals. *Advantage: DiRW ensures message aggregation among nodes with the same label, equivalent to data augmentation and highlighting label-specific positive signals for prediction.* (3) **Path-based Message Aggregation**. Based on the above homophily-aware paths, DiPathGNNs aggregate these messages for predicting each node through a learnable mechanism. *Advantage: DiRW facilitates the dense aggregation of direction-aware homophilous information, thus enhancing node prediction.*

Despite recent advancements in PathGNNs [17, 41, 51], their walk strategies are tailored for undirected graphs, lacking generalizability. Furthermore, the complex relationships inherent in directed

Permission to make digital or hard copies of all or part of this work for personal or classroom use is granted without fee provided that copies are not made or distributed for profit or commercial advantage and that copies bear this notice and the full citation on the first page. Copyrights for components of this work owned by others than ACM must be honored. Abstracting with credit is permitted. To copy otherwise, or republish, to post on servers or to redistribute to lists, requires prior specific permission and/or a fee. Request permissions from permissions@acm.org.
Conference'17, July 2017, Washington, DC, USA

© 2024 Association for Computing Machinery.
ACM ISBN 978-x-xxxx-xxxx-x/YY/MM...\$15.00
<https://doi.org/10.1145/nnnnnnnn.nnnnnnnn>

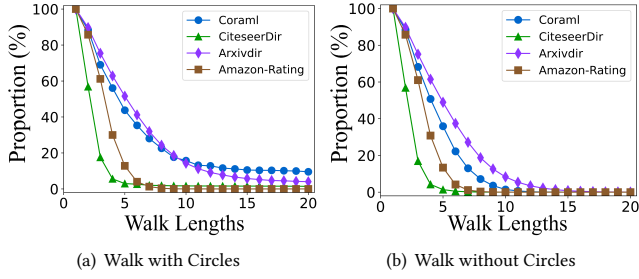


Figure 1: Interruption issue of DiSRW on digraphs.

topology pose unique challenges to the naive random walks, necessitating further investigations to develop fine-grained walk rules. To further elucidate, we present empirical analyses in Fig. 1(a)-2(b) that demonstrate these limitations and offer key insights.

(1) L1: Neglect of edge directions. Existing PathGNNs often fail to account for the edge direction. Utilizing directed simple random walks (DiSRW) on digraphs inevitably leads to interruptions when encountering nodes with no outgoing edges. To investigate and visualize this limitation, we employ DiSRW and initiate a walk from each node on four digraphs. As the walk length increases, we record the proportion of complete paths out of the total sequences, as depicted in Fig. 1(a). To mitigate the impact of cycles within the digraph, we also devise an DiSRW that excludes cycles and conduct the same experiment, as shown in Fig. 1(b).

Key Insight 1: *Walking strictly along the edge directions leads to severe walk interruption problems.* Due to the non-strongly connected nature of digraphs, most walks exhibit a sharp decline in the proportion of complete paths after only five steps. This indicates that the majority of walk sequences fail to gather extensive information beyond the immediate neighborhood of the originating node. Furthermore, when the influence of cycles is removed, the proportion of uninterrupted sequences declines more significantly.

(2) L2: Coarse-grained walk strategies. Most PathGNNs treat walk number and length as hyperparameters, uniformly applying them across all nodes. This one-size-fits-all approach overlooks the distinct contexts of nodes within complex topology. To further investigate this, we conducted an in-depth analysis of the effects of varying walk numbers (Fig. 2(a)) and walk lengths (Fig. 2(b)). Our evaluation is based on the undirected SRW, detailed in Appendix A.1. We categorized the top 50% homophilous nodes as homophily, while the remaining nodes were classified as heterophily.

Key Insight 2: *From the perspective of walk number, higher walk numbers can facilitate the prediction of heterophilous nodes.* Despite an increase in walk number providing no significant performance boost for homophilous nodes, it substantially enhances predictions for heterophilous nodes. Specifically, with fewer walks, low-homophily nodes fail to capture sufficiently structural insights. Consequently, increasing the number of walks allows for a more comprehensive exploration of a node’s intricate topological contexts. Conversely, nodes with high homophily exhibit a more uniform neighborhood structure, which can be accurately represented with fewer walks, as their local context is abundant in high-quality information. However, excessive walks in such case raise concerns regarding over-smoothing and time and space complexity.

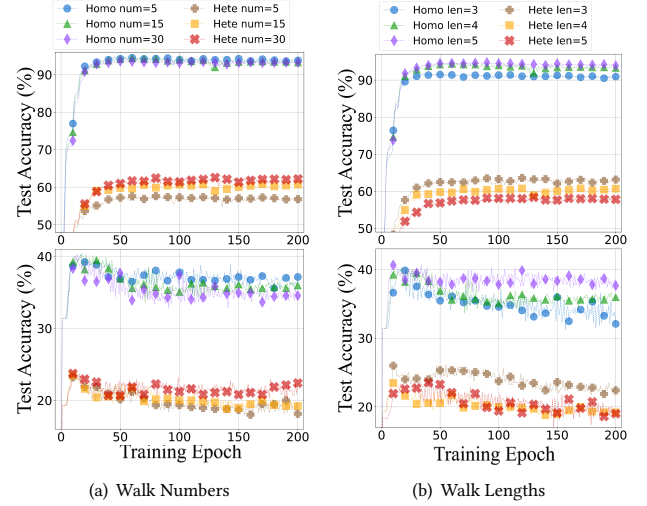


Figure 2: Performance on node classification tasks in digraph CiteseerDir (Homophilous, 3.3k Nodes, at Upper tables) and Actor (Heterophilous, 7.6k Nodes, at Lower tables).

Key Insight 3: *From the perspective of walk length, extending walk length positively affects nodes with high homophily but negatively impacts those with low homophily.* The underlying cause is rooted in the varying informational landscape depending on the homophily level of nodes. Nodes with low homophily are often surrounded by a noisy environment, where longer walks risk incorporating excessive irrelevant information and distracting features. Conversely, nodes with high homophily are typically surrounded by a more cohesive and informative neighborhood. In such contexts, longer walks are more beneficial as they include a broader spectrum of relevant information, providing the model with a more comprehensive view of the node’s surroundings.

Inspired by the above key insights, in this paper, we propose Directed Random Walk (DiRW), which can be viewed as a plug-and-play directed walk strategy for existing DiPathGNNs or a new learning paradigm for digraphs. Specifically, DiRW first designs a direction-aware walk strategy to identify potential relationships between the current node and its generalized neighbors through walk sequences (motivated by **Key Insight 1**). Subsequently, DiRW fine-tunes the walk numbers and walk lengths on a node-adaptive basis, thereby providing a rich information source for representing the current node (motivated by **Key Insight 2 & 3**). After that, DiRW employs a node-wise learnable path aggregator to efficiently represent node embeddings, which breaks the fixed neighborhood constraints of traditional message-passing mechanisms, allowing the exploration of higher-order node semantic consensus.

Our contributions. (1) *Novel Perspective.* To the best of our knowledge, this paper is the first to propose the concept of DiPathGNN and summarize its advantages. Furthermore, we emphasize the critical need for fine-grained walking strategies in digraphs, offering valuable empirical studies. (2) *Plug-and-play Strategy.* We introduce DiRW for digraphs, which customizes walk probabilities, length, and number for each node. It can be seamlessly integrated with any DiPathGNN to enhance performance. (3) *New DiGNN.* DiRW is also regarded as a new learning architecture for digraphs, consisting of an optimized path sampler in the pre-processing stage

and a well-designed node-wise path aggregator in the learning process. (4) *SOTA Performance*. Experiments demonstrate that DiRW achieves an improvement of 2.81% as a plug-and-play strategy in node classification and 0.82% as a novel DiGNN in link prediction.

2 PRELIMINARIES

2.1 Notation

We consider a digraph $\mathcal{G} = (\mathcal{V}, \mathcal{E})$ with $|\mathcal{V}| = n$ nodes and $|\mathcal{E}| = m$ edges. Each node has a feature vector of size f and a one-hot label of size c , with the feature and label matrices represented as $\mathbf{X} \in \mathbb{R}^{n \times f}$ and $\mathbf{Y} \in \mathbb{R}^{n \times c}$, respectively. The digraph \mathcal{G} can be described by an asymmetrical adjacency matrix \mathbf{A} , where $\mathbf{A}(u, v) = 1$ if $(u, v) \in \mathcal{E}$, and $\mathbf{A}(u, v) = 0$ otherwise. Suppose \mathcal{V}_l is the labeled set, and the goal of the semi-supervised node classification task is to predict the labels for nodes in the unlabeled set \mathcal{V}_u with the supervision of \mathcal{V}_l .

2.2 Directed Graph Neural Networks

2.2.1 Spatial-based Methods. To capture the asymmetric topology of digraphs, some spatial-based methods follow the strict symmetric message passing paradigm in the undirected setting [9, 15, 52, 58]. However, it is crucial to account for the directionality of the edges when aggregating messages. Specifically, for the current node $u \in \mathcal{V}$, the model learns weights to combine the representations of its out-neighbors ($u \rightarrow v$) and in-neighbors ($v \rightarrow u$) independently:

$$\begin{aligned} \mathbf{H}_{u \rightarrow}^{(l)} &= \text{Agg} \left(\mathbf{W}_{\rightarrow}^{(l)}, \text{Prop} \left(\mathbf{X}_u^{(l-1)}, \left\{ \mathbf{X}_v^{(l-1)}, \forall (u, v) \in \mathcal{E} \right\} \right) \right), \\ \mathbf{H}_{u \leftarrow}^{(l)} &= \text{Agg} \left(\mathbf{W}_{\leftarrow}^{(l)}, \text{Prop} \left(\mathbf{X}_u^{(l-1)}, \left\{ \mathbf{X}_v^{(l-1)}, \forall (v, u) \in \mathcal{E} \right\} \right) \right), \\ \mathbf{X}_u^{(l)} &= \text{Com} \left(\mathbf{W}^{(l)}, \mathbf{X}_u^{(l-1)}, \mathbf{H}_{u \rightarrow}^{(l)}, \mathbf{H}_{u \leftarrow}^{(l)} \right). \end{aligned} \quad (1)$$

Building upon this strategy, recent advances in digraph GNNs have further refined the message passing scheme to capture the inherent directionality of the digraph. For instance, DGCN [45] incorporates both first- and second-order neighbor proximity into the message aggregation process. DIMPA [13] expands the receptive field of by aggregating features from K -hop neighborhoods at each layer, enabling the capture of long-range dependencies. Inspired by the 1-WL graph isomorphism test, NSTE [19] tailors the message propagation to the directed nature of the graph. DiGCN [44] leverages neighbor proximity to increase the receptive field and proposes a digraph Laplacian based on personalized PageRank. ADPA [40] adaptively explores appropriate directed patterns to conduct weight-free graph propagation and employs two hierarchical node-wise attention mechanisms to obtain optimal node embeddings.

2.2.2 Spectral-based Methods. Spectral-based approaches for the DiGNN depart from the strict symmetric message passing used for undirected graphs [12, 49]. The core of spectral-based DiGNNs is to leverage a symmetric or conjugated digraph Laplacian \mathbf{L}_d , which is constructed based on the directed adjacency matrix \mathbf{A}_d . This symmetric Laplacian \mathbf{L}_d allows the application of spectral convolution operations, which can be formally represented as a function of the eigenvalues and eigenvectors of \mathbf{L}_d . Specifically, the layer-wise node embeddings $\mathbf{X}^{(l)}$ are computed via a first-order approximation of Chebyshev polynomials, leveraging the spectral

decomposition of the symmetric digraph Laplacian.

$$\begin{aligned} \mathbf{L}_d &= \text{DGS}(\mathbf{A}_d, \alpha, q), \\ \mathbf{X}^{(l+1)} &= \text{Poly}(\mathbf{L}_d) \text{MLP}(\mathbf{X}^{(l)}), \end{aligned} \quad (2)$$

where $\text{DGS}(\cdot)$ is the digraph generalized symmetric function with parameters and $\text{Poly}(\cdot)$ is a polynomial-based approximation method.

Building on this, DiGCN [44] proposes a α -parameterized stable state distribution based on the personalized PageRank to achieve the digraph convolution. MagNet [59] utilizes q -parameterized complex Hermitian matrix to model directed information in digraphs. MGC [56] adopts a truncated variant of PageRank, designing low-pass and high-pass filters tailored for homogeneous and heterogeneous digraphs. LightDiC [22] decouples graph propagation and feature aggregation for scalability in large-scale scenarios.

2.3 Path-based Graph Neural Networks

PathGNNs offer an effective approach to capture the intricate patterns within graphs by sampling and aggregating information along paths. For instance, GeniePath [25] introduces an adaptive path layer that intelligently navigates the exploration of both the breadth and depth of the node's receptive fields. SPAGAN [55] delves into the topological information of graphs by leveraging the shortest paths and applying path-based attention mechanisms to obtain node embeddings. PathNet [41] utilizes a maximal entropy-based random walk strategy to capture the heterophily information while preserving valuable structural information. RAWGNN [17] employs Node2Vec [11] to simulate both BFS and DFS, thereby capturing both homophily and heterophily information. PathMLP [51] designs a similarity-based path sampling strategy to capture smooth paths containing high-order homophily. The detailed descriptions of PathGNNs can be found in Appendix. A.8. We have also profoundly revealed that PathGNNs can be considered as a generalized and lightweight graph attention network in Appendix. A.9.

3 METHOD

Building upon the key insights discussed in Sec. 1, we now present our DiRW model, which is composed of two principal components: the optimized path sampler and the node-wise learnable path aggregator. The architecture of the model is depicted in Fig. 3.

Specifically, drawing upon **Key Insight 1**, DiRW is initiated with a direction-aware path sampling strategy in Sec. 3.1.1. This strategic approach determines the destinations for each walk step, thereby significantly augmenting the capacity to encapsulate the intricacies of directed topological structures. Furthermore, we introduce a multi-scale and multi-order walk probability scheme in Sec. 3.1.2, which models high-order and first-order homophily from both topological structure and node profiles. Guided by **Key Insight 3**, we customize the walk length for each path in Sec. 3.1.3. By introducing the homophily entropy, we evaluate the quality of walk sequences and terminate the walk when sequence quality reaches an optimal threshold. In Sec. 3.1.4, we propose a weight-free aggregation mechanism for the path embedding, which preserves the rich information encoded within the sequential order. Inspired by **Key Insight 2**, we tailor walk numbers in Sec. 3.1.5. By assessing the informational yield of sampled walks, we implement a stopping criterion that ensures the collection of ample yet efficient information,

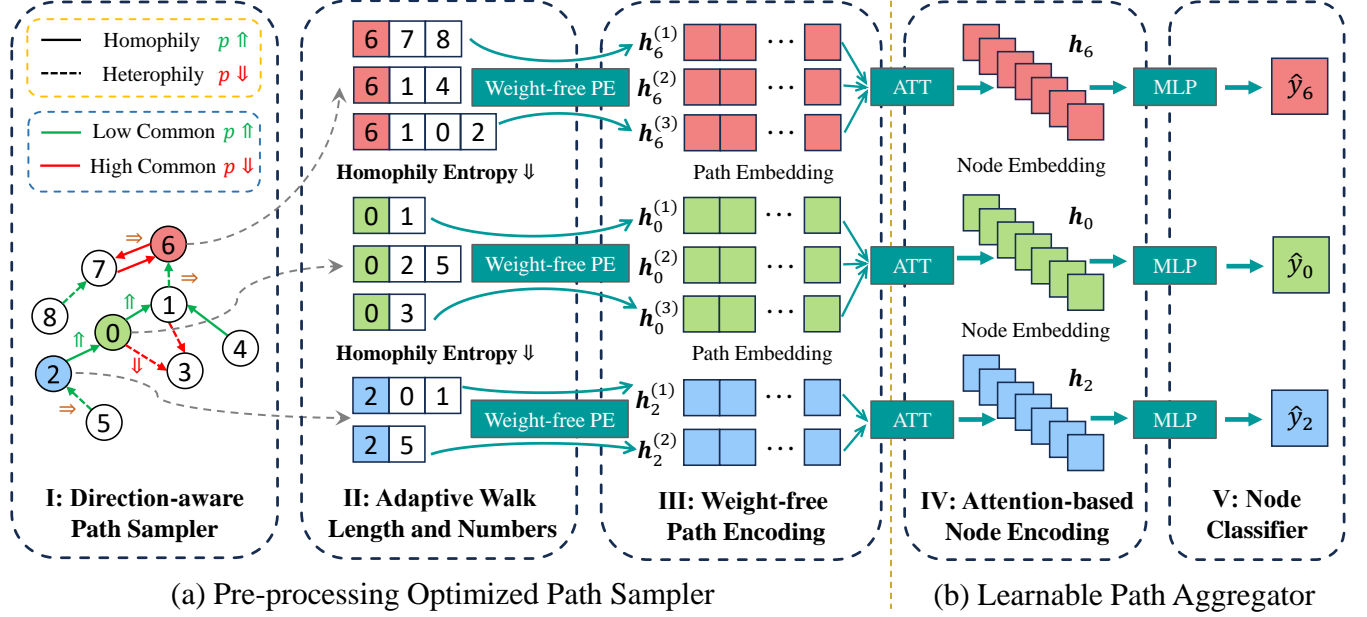


Figure 3: Overview of our DiRW, including (a) sample optimized sequences and calculate the path embeddings in a weight-free manner; (b) learn importance of different path to obtain accurate node predictions by node-wise path aggregator.

thereby optimizing the model’s performance. In the model learning phase, we integrate an attention mechanism to learn the importance of each walk sequence in Sec. 3.2.1, which prevents the aggregation of ineffective node information. Culminating in Sec. 3.2.2, we utilize a linear layer to distill the final node representations, which are applied to node classification and link prediction.

3.1 Optimized Path Sampler

3.1.1 Direction-aware Path Sampler. In DiRW, the direction of edges plays a pivotal role in the sampling process, dictating the trajectory of the random walk. This critical stage is tasked with determining the destination set for each step of the walk, which is essential for calculating the node probabilities and ensuring the continuity of the walk without interruptions.

Specifically, when the walk encounters a node that is devoid of incoming edges, the model strategically steers the walk towards its out-neighborhood. Conversely, if a node lacks outgoing edges, the walk remains confined to its in-neighborhood. This approach effectively circumvents the issue of walk termination at nodes with unidirectional connectivity, which is mentioned in **Key Insight 1**. For nodes that possess both incoming and outgoing edges, a more nuanced strategy is essential to balance the presence and directionality of edges. Drawing inspiration from the magnetic Laplacian matrix utilized for digraphs [59], DiRW introduces a hyperparameter $q \in [0, 1]$. At each walk step, a random value r is sampled uniformly from the $[0, 1]$. If r surpasses q , the walk proceeds along the directed edge, anchoring the target node within the out-neighbors. Otherwise, the walk considers both the in-neighbors and out-neighbors of the node. The formulation of this process is

encapsulated in the following equations:

$$\begin{aligned} D_u &= \mathbb{I}(A_u \cdot \mathbf{1} > 0), \\ P_u &= D_u \cdot (q \cdot A_u + (1 - q) \cdot (A_u + A_u^T)) + (1 - D_u) \cdot A_u^T, \end{aligned} \quad (3)$$

where $\mathbb{I}(\text{condition})$ is the indicate function, which equals 1 if the condition is met and 0 otherwise, and $\mathbf{1}$ is the vector of ones. D_u is a scalar that determines the presence of outgoing edges of node u . P_u represents the potential destinations matrix guiding the walk towards the next node in the sequence.

3.1.2 Multi-scale and Multi-order Walk Probability. The computation of walk probabilities in DiRW is a nuanced process that seamlessly blends topological structure with node profiles, which allows DiRW to delve into the complexities of both high-order and one-order homophily within heterophilous graphs.

From the topological perspective, DiRW is designed to unearth *high-order* homophily information which is often embedded within heterophilous graphs [51]. The model strategically prioritizes nodes which share a limited amount of common neighbors with the current node, bridging to distant regions of the digraph. The topological-based probability measure, denoted as P_u^{topo} , is crafted to be inversely proportional to the number of common neighbors $\text{Com}(u, v)$ and normalized by the degree $\text{Deg}(v)$ of the candidate node v .

$$P_u^{\text{topo}}(v) = 1 - \frac{\text{Com}(u, v) + 1}{\text{Deg}(v)}. \quad (4)$$

Additionally, from the feature standpoint, DiRW captures *one-order* homophily by favoring walks towards neighbors with more similar features, which present stronger homophily. The feature-based probability P_u^{feat} is calculated based on the cosine similarity between the features of the current node and candidate node.

$$P_u^{\text{feat}}(v) = \cos(X_u, X_v). \quad (5)$$

The transition probability from node u to node v in a walk step is determined by aggregating the topological- and feature-based probabilities, which are then normalized by a softmax function.

$$\mathbf{P}_u^{dst}(v) = \text{Softmax} \left(\left(\mathbf{P}_u^{topo}(v) + \mathbf{P}_u^{feat}(v) \right) \cdot \mathbb{I}(\mathbf{P}_u(v) > 0) \right). \quad (6)$$

Recognizing that the softmax scales vary with the walk directions, we pre-compute the topological- and feature-based probabilities (\mathbf{P}^{topo} and \mathbf{P}^{feat}) to obviate repetitive calculations and ensure the operational efficiency of our DiRW.

3.1.3 Homophily Entropy-based Personalized Walk Length. In DiRW, the walk length is not predefined but is instead dynamically tailored based on according to the homophily entropy. Traditional homophily metrics predominantly focus on immediate neighborhood information, providing a limited view of the walk sequence's quality. To address this limitation, we introduce a novel metric - *homophily entropy* - which evaluates the walk sequence quality through the lens of feature similarity among the nodes within the sequence. Our objective is to ensure that each node in the walk sequence maintains a strong homophilous relationship with the originating node, thereby enriching the aggregated information with relevance to it. To achieve this, we first convert the sampled path into a homophily label sequence, represented as follows:

$$p^{homo}(i) = \mathbb{I}(\mathbf{X}_{P(i)} \neq \mathbf{X}_{P(0)}) \cdot i, \quad (7)$$

where $P(i)$ and $p^{homo}(i)$ denotes the i -th element in the walk sequence and the homophily label sequence, respectively. By applying Shannon entropy [21] to it, we derive the homophily entropy:

$$H_{homo}(P) = H(p^{homo}) = - \sum_i p(i) \log p(i), \quad (8)$$

where $p(i)$ represents the probability of observing the i -th element in p^{homo} . Our analysis indicates that a lower homophily entropy corresponds to a higher quality walk sequence.

This metric is instrumental in guiding the determination of walk length for each sequence. We initiate by setting a minimum walk length l_{min} to guarantee the collection of adequate information. Upon reaching l_{min} , the walk is extended until two consecutive increases in homophily entropy are detected, signifying an encounter with a heterophilous neighborhood. It aligns with the **Key Insight 3** outlined in Sec. 1, as homophilous nodes prefer longer walks.

3.1.4 Weight-free Path Encoding. To account for the varying influence of nodes along a path, DiRW employs an exponential decay function to assign weights and compute the path embedding. This scheme preserves the order information in the sequence and ensures that nodes in proximity to the originating node in the path are accorded greater significance in the path embedding. The weight assigned to each node in the path is calculated as follows:

$$w_i = \frac{c^i}{\sum_{j=1}^k c^j}, \quad i = 1, 2, \dots, k, \quad (9)$$

where $c \in (0, 1)$ is the decay hyperparameter, and k denotes the length of the path. The path embedding is obtained by a weighted sum of the node features along the path, given by:

$$\mathbf{h}_u^{(j)} = \sum_{i=1}^k w_i \mathbf{X}_{P_u^{(j)}(i)}. \quad (10)$$

where $P_u^{(j)}$ and $\mathbf{h}_u^{(j)}$ represent the j -th sampled path and j -th path embedding of node u , respectively. This weight-free aggregation mechanism allows for the integration of the sampling into the pre-processing stage, which substantially reduces the computational complexity during training. Moreover, the exponential decay mechanism effectively retains the sequential information inherent in the walk sequence, surpassing the constraints of conventional message-passing approaches that often rely on uniform weighting.

3.1.5 Adaptive Walk Numbers. Ensuring the collection of comprehensive contextual information is critical in DiRW, guiding the determination of the requisite number of walks per node. This is achieved by evaluating the richness of information encapsulated within the path embeddings. The richness is quantified through the average embedding of the sampled paths, represented as:

$$\mathbf{z}_u^k = \frac{1}{k} \sum_{i=1}^k \mathbf{h}_u^{(i)}, \quad (11)$$

where k is the number of sampled paths. To avoid the premature termination of the walk process, an initial minimum walk number n_{min} is established. Subsequent to each walk, DiRW calculates the L2 norm of the discrepancy between the current measure of information richness and that of the preceding iteration:

$$\Delta = \|\mathbf{z}_u^k - \mathbf{z}_u^{k-1}\|_2, \quad k > n_{min}. \quad (12)$$

If the value of Δ fall below the predefined threshold δ , it indicates that the sampling has reached a saturation point, beyond which additional walks are unlikely to contribute substantially to the information richness. In such cases, the walk is discontinued to prevent further unnecessary and redundant sampling, which enhances the efficiency of the information gathering process and is reflective of our **Key Insight 2**. It acknowledges that heterophilous nodes are often characterized by more intricate neighborhoods and necessitate a greater walk number to amass a sufficiently rich information.

3.2 Learnable Path Aggregator

3.2.1 Attention-based Node Encoding. Following the pre-processing sampling phase, the DiRW model harnesses an attention mechanism to discern and weigh the informativeness of various path embeddings. This process is pivotal for constructing node embeddings that are rich in relevant contextual information.

Specifically, for each node u , DiRW initiates the encoding of the sampled paths \mathbf{h}_u through a pair of linear layers, interspersed with a LeakyReLU activation function. The resulting encoding e_u is subsequently processed through a softmax function to yield attention scores α_u . The final node embedding \mathbf{z}_u is then computed as a weighted aggregation of the path embeddings $\mathbf{h}_u^{(i)}$, with the weights being the attention scores α_u^i , articulated as follows:

$$\begin{aligned} e_u &= \text{MLP}_2(\text{LeakyReLU}(\text{MLP}_1(\mathbf{h}_u))), \\ \alpha_u &= \text{Softmax}(e_u), \\ \mathbf{z}_u &= \sum_{i=1}^k \alpha_u^i \mathbf{h}_u^{(i)}. \end{aligned} \quad (13)$$

3.2.2 Node Classifier. With the node embeddings \mathbf{z}_u at hand, DiRW deploys an MLP to perform the node classification task, employing

Table 1: Model performance (%) as a DiGNN in node classification. The best result is bold. The second result is underlined.

Type	Models	CoraML	CiteSeer	WikiCS	Amazon Computers	Chameleon	Actor	Rating	Arxiv	Products	Rank
Undirected GNNs	GCN	84.48±0.17	65.26±1.07	78.98±0.49	83.26±0.51	40.93±1.24	30.96±0.45	43.37±0.13	67.80±0.07	73.3±0.07	5.67
	GAT	83.73±0.47	63.12±1.06	79.35±0.28	80.16±2.32	40.82±2.46	30.29±0.37	45.03±0.50	<u>67.79±0.24</u>	OOM	7.44
Spatial DiGNNs	DGCN	81.27±0.58	64.66±0.65	78.71±0.19	82.95±1.13	41.96±1.00	30.87±0.38	44.24±0.28	OOT	OOM	8.00
	NSTE	80.06±0.89	62.99±1.08	77.58±0.29	78.50±1.87	40.31±1.87	31.14±0.46	45.31±0.15	64.40±0.94	OOT	9.78
	DIMPA	79.77±0.66	60.88±1.08	78.58±0.27	77.80±1.42	40.41±1.88	30.84±0.73	41.58±0.17	65.89±0.22	72.89±0.13	10.67
	Dir-GNN	79.92±1.26	63.74±0.87	79.04±0.26	81.34±0.92	41.96±1.95	30.12±0.65	43.74±0.10	64.26±0.48	72.93±0.17	8.33
	ADPA	79.10±1.56	65.01±2.29	<u>79.43±0.92</u>	73.25±4.26	41.66±3.07	35.29±0.82	44.90±0.62	64.28±0.56	OOT	7.67
Spectral DiGNNs	DiGCN	80.81±0.52	62.38±0.28	79.30±0.32	80.02±1.52	41.24±1.67	34.30±0.89	<u>45.99±0.28</u>	65.38±0.47	OOM	7.11
	DiGCNapp	80.65±0.40	62.05±0.59	78.54±0.32	81.53±1.27	40.93±2.49	30.99±0.49	40.46±0.20	61.57±0.56	73.51±0.05	9.33
	MagNet	80.45±0.46	<u>65.63±1.69</u>	79.19±0.20	<u>83.41±0.99</u>	<u>42.78±0.63</u>	31.39±0.53	45.97±0.71	68.22±0.25	<u>74.21±0.06</u>	3.78
	MGC	82.66±1.01	64.78±1.05	77.42±0.28	81.26±0.80	41.34±3.29	35.75±0.41	42.01±0.36	66.73±0.17	59.86±3.20	7.11
	LightDiC	82.67±1.10	64.36±0.35	78.02±0.21	79.87±0.68	42.68±1.61	30.59±0.50	40.53±0.48	63.41±0.26	64.85±0.07	8.78
PathGNNs	RAW-GNN	78.35±0.90	59.94±0.38	76.76±0.31	72.76±0.67	41.24±3.34	34.71±0.80	44.07±0.32	OOM	OOM	11.89
	PathNet	66.61±6.83	61.41±1.93	75.71±0.66	68.78±2.13	38.44±3.21	36.67±0.92	39.15±0.40	OOM	OOM	13.22
	DiRW	<u>84.24±0.19</u>	65.88±1.41	79.87±0.08	83.50±0.68	43.92±0.23	<u>36.42±0.46</u>	46.13±0.39	68.51±0.18	75.19±0.47	1.22

Table 2: Model Performance (%) as a plug-and-play strategy on PathGNNs in node classification.

Models	CoraML	CiteSeer	WikiCS	Amazon Computers	Chameleon	Actor	Rating	Improvement
RAWGNN	78.35±0.90	59.94±0.38	76.76±0.31	72.76±0.67	41.24±3.34	34.71±0.80	44.07±0.32	
RAWGNN+DiRW	82.67±0.26	64.54±0.75	77.71±0.27	76.33±1.02	43.30±1.31	35.55±0.39	45.66±0.63	↑ 4.34%
PathNet	66.61±6.83	61.41±1.93	75.71±0.66	68.78±2.13	38.44±3.21	36.67±0.92	39.15±0.40	
PathNet+DiRW	68.25±0.77	62.66±0.89	76.21±0.35	69.45±0.97	38.88±1.04	37.14±0.87	39.22±0.24	↑ 1.25%
DiRW	84.24±0.19	65.88±1.41	79.87±0.08	83.50±0.68	43.92±0.23	36.42±0.46	46.13±0.39	—

the cross-entropy loss function to guide the training process:

$$\hat{y}_u = \text{Softmax}(\text{MLP}_3(\mathbf{z}_u)),$$

$$\mathcal{L} = -\frac{1}{|\mathcal{V}_l|} \sum_{i \in \mathcal{V}_l} Y_i \log \hat{y}_i, \quad (14)$$

where \mathcal{V}_l represents the set of labeled training nodes. $Y_i \in \mathbb{R}^c$ and $\hat{y}_i \in \mathbb{R}^c$ correspond to the one-hot encoded true label and the predicted label for node i , respectively.

4 EXPERIMENTS

In this section, we conduct thorough evaluations of our DiRW. Our experiments are structured to answer four pivotal questions: **Q1**: Can DiRW achieve superior performance as a new DiGNN and as a plug-and-play strategy for existing PathGNNs? **Q2**: If DiRW proves to be effective, what factors contribute to its enhanced performance? **Q3**: What is the running efficiency of DiRW? **Q4**: How is the path quality of DiRW and other PathGNNs? To maximize the usage for the space, we introduce datasets, baselines, experimental settings in Appendix A.2-A.5, demonstrate the results of link-level tasks in Appendix A.6, and include a sensitivity analysis in Appendix A.7.

4.1 Overall Performance

4.1.1 An Innovative Learning Architecture. To answer **Q1**, we conduct comparative experiments to evaluate the performance of DiRW in node classification. The results presented in Tab. 1 demonstrate that as a novel DiGNN, DiRW achieves exceptional performance

across all datasets and outperforms the current leading DiGNN MagNet by an average of 3.2%, which is attributed to its adept modeling of digraphs and heterophilous relationships. In contrast, traditional undirected GNNs perform well in homophilous scenarios but struggle in heterophilous digraphs due to simplistic undirected adjacency matrix approaches. Moreover, while Dir-GNN and ADPA strive to tackle heterophily with digraph modeling, their methods show limitations in effectively generalizing to homophilous digraphs. Furthermore, while undirected PathGNNs show promise in modeling heterophilous graphs, their performance is significantly hindered by critical shortcomings. Notably, these models fail to account for the directionality of edges in digraphs, and their simplistic walk strategies limit their effectiveness in complex digraph structures.

It is imperative to highlight that the sophisticated model architectures such as RNNs employed in PathGNNs engender scalability challenges, leading to out-of-memory (OOM) errors when dealing with large-scale digraphs ogbn-arxiv and ogbn-products. Similarly, the intricate message-passing paradigms that incorporate multiple convolutional layers in DGCN and NSTE result in incomplete training within 12 hours, culminating in out-of-time (OOT) errors. In contrast, DiRW revels in its high efficiency and achieves superior performance on large-scale digraphs with its weight-free path sampling strategy and lightweight learning mechanism.

4.1.2 A Plug-and-Play Approach. Beyond assessing DiRW as an innovative neural architecture, we also integrate the optimized path

Table 3: Ablation study performance (%).

Models	CiteSeer	WikiCS	Chameleon	Rating
w/o Dir	65.11±1.77	79.65±0.18	42.47±1.07	45.59±0.16
w/o Topo	64.26±0.17	79.37±0.13	38.97±2.64	45.79±0.18
w/o Feat	65.77±1.28	79.27±0.13	41.65±1.73	45.62±0.25
w/o Att	65.02±0.75	79.26±0.32	39.59±2.23	42.55±0.39
DiRW-Gate	65.65±0.84	79.52±0.28	38.76±3.56	42.68±0.15
DiRW-JK	63.88±1.02	79.31±0.25	40.21±3.82	42.74±0.33
DiRW	65.88±1.41	79.87±0.08	43.92±0.23	46.13±0.39

sampler with other PathGNNs. Specifically, we combine DiRW with RAWGNN and PathNet to enable modeling of digraphs. Due to the complicated path and node embedding learning rules designed in these two models, it is tough for the weight-free adaptive walking length and number in DiRW to generalize to them. Therefore, we have incorporated only the direction-aware sampling strategy and the walking probabilities that consider both topological structure and node profiles into these two models to explore their performances. The results are demonstrated in Tab. 2.

The results offer compelling evidence that the optimized path sampler we have carefully developed for digraphs substantially improves the performance of both RAWGNN and PathNet. The performance gains can be directly linked to the shortcomings of the original PathGNNs, which did not adequately consider the directionality of edges in digraphs, leading to a substantial loss of valuable information. DiRW addresses this shortcoming by balancing the directionality and existence of directed edges into the sampling process, thereby effectively capturing the intricate topological structures present in digraphs. In addition, our walking probabilities which take into account both the topological structure and the node profiles have demonstrated superior performance compared to RAW-GNN and PathNet that solely considered the topology in their walking probability design. By modeling node similarity, DiRW effectively captures one-hop homophily information in heterophilous settings. The successful integration of these two strengths has not only led to improved performance when DiRW is considered as a plug-and-play module with other PathGNNs but also underscores the adaptability and robustness of our approach.

4.2 Ablation Study

To answer Q2, we have conducted a series of ablation studies to ascertain the individual contributions of the six core components that constitute the backbone of DiRW. Starting with the direction-aware path sampler, we set the walk direction coefficient q to 1 to simulate a sampling scenario without directionality (w/o Dir). Next, we conducted separate ablations for the topological-based (w/o Topo) and feature-based (w/o Feat) walk probabilities to understand the relative importance of node profiles and topological structure in guiding the walks. Additionally, the ablation experiment for our node-wise attention mechanisms is conducted, which is replaced by directly averaging path embeddings (w/o Att), Gate attention proposed by [1] (DiRW-Gate) and JK attention proposed by [52] (DiRW-JK). The outcomes of these ablation studies are detailed in Tab. 3. Furthermore, to evaluate the adaptive walk length and numbers, we replace them with fixed hyperparameters and depict the outcomes in Fig. 4. We measured the performance and running

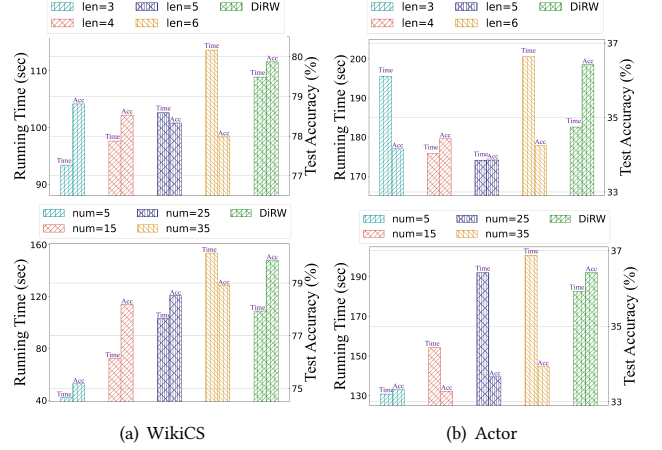


Figure 4: Performance and running time of DiRW and its variants of without adaptive walk length (Upper) and without personalized walk number (Lower).

time under varying walk lengths and number, while keeping other hyperparameters consistent with DiRW to ensure a fair comparison. We draw the following conclusions from the results:

Direction-aware path sampler. By effectively balancing the directionality and existence of edges in digraphs, the direction-aware path sampler has significantly enhanced the model’s capacity to capture the intricate topological structures of digraphs, thereby resulting in an average performance improvement of 1.5%.

Topological walk probability. Designed to facilitate exploration of high-order homophilous neighbors, the topological-based walk probabilities have demonstrated a marked advantage in detecting homophilous patterns within the digraphs, contributing to notable enhancements in the model’s predictive performance.

Feature-based walk probability. By harnessing node profiles to guide the exploration towards nodes with strong homophilous ties, the feature-based walk probability has successfully driven an average performance increase of 1.9%, highlighting the critical role of feature information in guiding walk preference.

Node-wise Learnable Path Aggregator. By employing our nuanced attention mechanism to discern the salience of different paths, DiRW adeptly differentiates between effective and ineffective sampling sequences, thereby distilling high-quality node embeddings and results in an average performance boost of 5.36%. The node-wise attention mechanism excels by integrating a dual MLP, which is adept at capturing complex and subtle nuances in the path embeddings as compared to the single MLP used in the JK and Gate attention mechanisms. The dual-layer MLP not only processes the initial linear transformation of the path embeddings but also applies a subsequent layer that refines the feature representation.

Homophily entropy-based personalized walk length. The personalized walk length has proven to be a boon for DiRW performance, outclassing any model reliant on a static walk length. Traditional approaches with longer fixed walk length often necessitate substantial pre-processing time and yield sub-optimal performances. In contrast, DiRW achieves a commendable efficiency and optimal effectiveness. By leveraging homophily entropy to assess the path quality, DiRW is adept at identifying and sampling

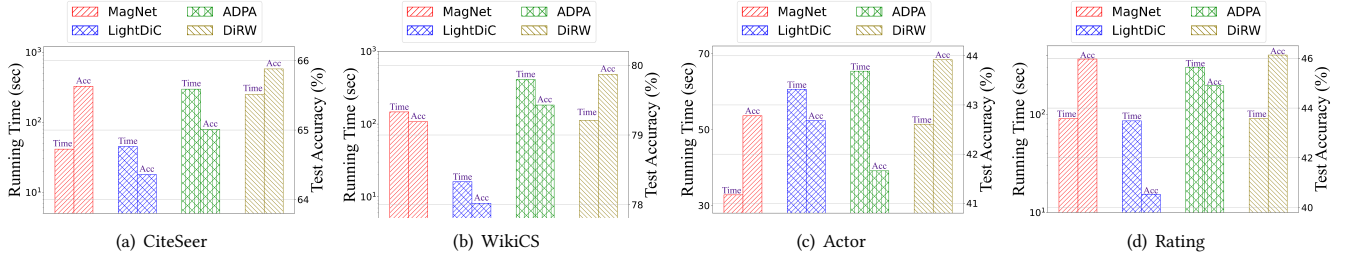


Figure 5: Accuracy and efficiency performance of DiRW and other DiGNNs.

high-quality sequences promptly, thus streamlining the sampling process and ensuring that the model operates at an optimal level.

Heuristic adaptive walk number. Echoing the success of the personalized walk length, the heuristic adaptive walk number also demonstrates a significant performance improvement over models that utilize a rigid number of walks. This superior efficiency and effectiveness stems from our systematic evaluation of the information richness within sampled walks, allowing the model to sample a informative set of walk sequences in a shorter span.

4.3 Efficiency Analysis

To address Q3, we conducted experiments to evaluate the efficiency of DiRW. We selected an spatial-based baseline ADPA and two spectral-based baselines Magnet and LightDiC to benchmark their performance and efficiency. The metric for efficiency was established based on the total time required to run each model for five times, with the results graphically depicted in Fig. 5.

From the visual representation, it is evident that the superiority of DiRW lies in both predictive accuracy and operational efficiency. Despite the variability in the optimal adaptive walk length and walk numbers across different datasets, which might introduce some instability in computational time, DiRW maintains an acceptable time cost and consistently outperforms ADPA. The result reveals that ADPA is consistently the most time-consuming model. This is largely due to its intricate architecture, featuring hierarchical attention mechanisms and multiple convolution layers, which increases its computational complexity and resource requirements.

Significantly, the majority of DiRW’s running time is consumed by the sampling stage, which can be a bottleneck in the overall training process. However, by pre-processing this sampling stage and storing the sequences, which is similar to the approach employed by PathNet, we can considerably enhance the efficiency of the training pipeline. Furthermore, DiRW’s rapid learning mechanism is designed to leverage these pre-processed sequences effectively, facilitating a more streamlined and accelerated training process.

4.4 Path Quality Analysis

To answer Q4, we conducted an in-depth analysis comparing the path quality sampled by our optimized path sampler with those generated by the DFS and BFS utilized in RAWGNN. This analysis is examined by the homophily entropy according to Eq. (8).

The experimental outcomes in Fig. 6 demonstrate that the paths sampled by DiRW consistently exhibit lower homophily entropy compared to those produced by DFS and BFS. This superiority is

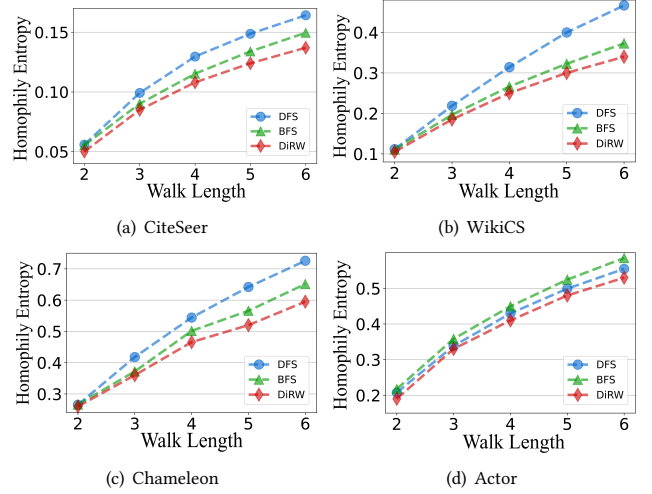


Figure 6: Path Homophily Entropy Comparison.

primarily attributed to the integrated consideration of both topological structure and node profiles in walk probability mechanism, coupled with the adaptive walk length guided by homophily entropy. Furthermore, the DFS approach demonstrated the highest homophily entropy in most scenarios. This can be attributed to the fact that BFS, with its mechanism of exploring the immediate neighborhood, aligns well with the homophily assumption. However, in scenarios characterized by strong heterophily like actor, DFS outperforms BFS in path sampling quality. Our DiRW model achieves a harmonious balance between these two approaches, leveraging the strengths of both while mitigating their respective weaknesses.

5 CONCLUSION AND FUTURE WORK

In this work, we have underscored the necessity of DiGNNs in the context of modern graph-structured data and proposed DiPathGNN mechanism to capture the inherent homophilous information in digraphs. Through empirical analysis, we have exposed the limitations of current PathGNNs, particularly in their lack of edge direction modeling and coarse-grained sampling strategy. To address these challenges, we propose DiRW, a novel path-aware digraph learning approach. DiRW is distinguished by its direction-aware path sampler, which is meticulously fine-tuned based on walk probability, length, and numbers in a weight-free approach. Furthermore, DiRW employs a node-wise learnable path aggregator to formulate nuanced node representations. Experiments demonstrate that

DiRW achieves SOTA performance in node- and link-level tasks, especially for topologically heterophilous scenarios.

Looking ahead, there are several promising directions for future research. First, we aim to explore more efficient sampling strategies that can further enhance the training effectiveness. Furthermore, developing adaptive sampling methods that dynamically adjust based on the characteristics of the graph could potentially improve the performance and scalability of our approach. Lastly, designing better learning mechanisms to capture the complex relationships between nodes in digraphs could lead to more accurate predictions. These future works will further enhance our understanding of digraph learning and potentially lead to breakthroughs in how we model and analyze complex graph-structured data.

REFERENCES

- [1] Wasi Uddin Ahmad, Nanyun Peng, and Kai-Wei Chang. 2021. GATE: graph attention transformer encoder for cross-lingual relation and event extraction. In *Proceedings of the Association for the Advancement of Artificial Intelligence, AAAI*.
- [2] Usman Ahmed, Jerry Chun-Wei Lin, and Gautam Srivastava. 2022. Hyper-Graph Attention Based Federated Learning Method For Mental Health Detection. *IEEE Journal of Biomedical and Health Informatics* (2022).
- [3] Takuya Akiba, Shotaro Sano, Toshihiko Yanase, Takeru Ohta, and Masanori Koyama. 2019. Optuna: A next-generation hyperparameter optimization framework. In *Proceedings of the ACM SIGKDD Conference on Knowledge Discovery and Data Mining, KDD*.
- [4] Vicente Balmaseda, María Coronado, and Gonzalo de Cadenas-Santiago. 2023. Predicting Systemic Risk in Financial Systems Using Deep Graph Learning. *Intelligent Systems with Applications* (2023), 200240.
- [5] Aleksandar Bojchevski and Stephan Günnemann. 2018. Deep Gaussian Embedding of Graphs: Unsupervised Inductive Learning via Ranking. In *ICLR Workshop on Representation Learning on Graphs and Manifolds*.
- [6] Shaked Brody, Uri Alon, and Eran Yahav. 2022. How attentive are graph attention networks? *International Conference on Learning Representations, ICLR* (2022).
- [7] Xuheng Cai, Chao Huang, Lianghao Xia, and Xubin Ren. 2023. LightGCL: Simple Yet Effective Graph Contrastive Learning for Recommendation. In *International Conference on Learning Representations, ICLR*.
- [8] Thomas M Cover. 1999. *Elements of information theory*. John Wiley & Sons.
- [9] Fabrizio Frasca, Emanuele Rossi, Davide Eynard, Ben Chamberlain, Michael Bronstein, and Federico Monti. 2020. Sign: Scalable inception graph neural networks. *arXiv preprint arXiv:2004.11198* (2020).
- [10] Edouard Grave, Piotr Bojanowski, Prakhar Gupta, Armand Joulin, and Tomas Mikolov. 2018. Learning word vectors for 157 languages. *arXiv preprint arXiv:1802.06893* (2018).
- [11] Aditya Grover and Jure Leskovec. 2016. Node2vec: Scalable Feature Learning for Networks. In *Proceedings of the ACM SIGKDD Conference on Knowledge Discovery and Data Mining, KDD*.
- [12] Mingguo He, Zhewei Wei, Hongteng Xu, et al. 2021. Bernnet: Learning arbitrary graph spectral filters via bernstein approximation. *Advances in Neural Information Processing Systems, NeurIPS* (2021).
- [13] Yixuan He, Gesine Reinert, and Mihai Cucuringu. 2022. DIGRAC: Digraph Clustering Based on Flow Imbalance. In *Learning on Graphs Conference, LoG*.
- [14] Weihua Hu, Matthias Fey, Marinka Zitnik, Yuxiao Dong, Hongyu Ren, Bowen Liu, Michele Catasta, and Jure Leskovec. 2020. Open graph benchmark: Datasets for machine learning on graphs. *Advances in Neural Information Processing Systems, NeurIPS* (2020).
- [15] Qian Huang, Horace He, Abhay Singh, Ser-Nam Lim, and Austin R Benson. 2021. Combining label propagation and simple models out-performs graph neural networks. *International Conference on Learning Representations, ICLR* (2021).
- [16] Woochang Hyun, Jaehong Lee, and Bongwon Suh. 2023. Anti-Money Laundering in Cryptocurrency via Multi-Relational Graph Neural Network. In *Pacific-Asia Conference on Knowledge Discovery and Data Mining*. Springer, 118–130.
- [17] Di Jin, Rui Wang, Meng Ge, Dongxiao He, Xiang Li, Wei Lin, and Weixiong Zhang. 2022. RAW-GNN: RANdom Walk Aggregation based Graph Neural Network. In *Proceedings of the International Joint Conference on Artificial Intelligence, IJCAI*.
- [18] Thomas N Kipf and Max Welling. 2017. Semi-supervised classification with graph convolutional networks. In *International Conference on Learning Representations, ICLR*.
- [19] Georgios Kollias, Vasileios Kalantzis, Tsuyoshi Idé, Aurélie Lozano, and Naoki Abe. 2022. Directed Graph Auto-Encoders. In *Proceedings of the Association for the Advancement of Artificial Intelligence, AAAI*.
- [20] Jure Leskovec and Andrej Krevl. 2014. SNAP Datasets: Stanford large network dataset collection. (2014).
- [21] Angsheng Li and Yicheng Pan. 2016. Structural information and dynamical complexity of networks. *IEEE Transactions on Information Theory* 62, 6 (2016), 3290–3339.
- [22] Xunkai Li, Meihao Liao, Zhengyu Wu, Daohan Su, Wentao Zhang, Rong-Hua Li, and Guoren Wang. 2024. LightDiC: A Simple yet Effective Approach for Large-scale Digraph Representation Learning. *arXiv preprint arXiv:2401.11772* (2024).
- [23] Xunkai Li, Jingyuan Ma, Zhengyu Wu, Daohan Su, Wentao Zhang, Rong-Hua Li, and Guoren Wang. 2024. Rethinking Node-wise Propagation for Large-scale Graph Learning. In *Proceedings of the ACM Web Conference, WWW*.
- [24] Jiaxuan Liang, Jun Wang, Guoxian Yu, Wei Guo, Carlotta Domeniconi, and Maozu Guo. 2023. Directed acyclic graph learning on attributed heterogeneous network. *IEEE Transactions on Knowledge and Data Engineering* (2023).
- [25] Ziqi Liu, Chaochao Chen, Longfei Li, Jun Zhou, Xiaolong Li, Le Song, and Yuan Qi. 2019. Geniepath: Graph neural networks with adaptive receptive paths. In *Proceedings of the AAAI conference on artificial intelligence*, Vol. 33. 4424–4431.
- [26] Sitao Luan, Chenqing Hua, Qincheng Lu, Jiaqi Zhu, Mingde Zhao, Shuyuan Zhang, Xiao-Wen Chang, and Doina Precup. 2022. Revisiting heterophily for graph neural networks. *Advances in Neural Information Processing Systems, NeurIPS* (2022).
- [27] Yuankai Luo, Veronika Thost, and Lei Shi. 2023. Transformers over Directed Acyclic Graphs. *Advances in Neural Information Processing Systems, NeurIPS* (2023).
- [28] Yao Ma, Xiaorui Liu, Neil Shah, and Jiliang Tang. 2021. Is homophily a necessity for graph neural networks? *International Conference on Learning Representations, ICLR* (2021).
- [29] Seiji Maekawa, Yuya Sasaki, and Makoto Onizuka. 2023. Why Using Either Aggregated Features or Adjacency Lists in Directed or Undirected Graph? Empirical Study and Simple Classification Method. *arXiv preprint arXiv:2306.08274* (2023).
- [30] Péter Mernyei and Cătălina Cangea. 2020. Wiki-CS: A Wikipedia-Based Benchmark for Graph Neural Networks. *arXiv preprint arXiv:2007.02901* (2020).
- [31] Hongbin Pei, Bingzhe Wei, Kevin Chen-Chuan Chang, Yu Lei, and Bo Yang. 2020. Geom-gcn: Geometric graph convolutional networks. In *International Conference on Learning Representations, ICLR*.
- [32] Jeffrey Pennington, Richard Socher, and Christopher D Manning. 2014. Glove: Global vectors for word representation. In *Proceedings of Conference on Empirical Methods in Natural Language Processing, EMNLP*.
- [33] Bastian Pfeifer, Anna Saranti, and Andreas Holzinger. 2022. GNN-SubNet: disease subnetwork detection with explainable graph neural networks. *Bioinformatics* 38, Supplement_2 (2022), ii120–ii126.
- [34] Oleg Platonov, Denis Kuznedelev, Michael Diskin, Artem Babenko, and Liudmila Prokhorenkova. 2023. A critical look at the evaluation of GNNs under heterophily: are we really making progress? *International Conference on Learning Representations, ICLR* (2023).
- [35] Yuxin Qiu. 2023. Default Risk Assessment of Internet Financial Enterprises Based on Graph Neural Network. In *IEEE Information TechnoLoGy, Networking, Electronic and Automation Control Conference*, Vol. 6. IEEE, 592–596.
- [36] Emanuele Rossi, Bertrand Charpentier, Francesco Di Giovanni, Fabrizio Frasca, Stephan Günnemann, and Michael Bronstein. 2023. Edge Directionality Improves Learning on Heterophilic Graphs. In *Proceedings of The European Conference on Machine Learning and Principles and Practice of Knowledge Discovery in Databases, ECML-PKDD Workshop* (2023).
- [37] Benedek Rozemberczki, Carl Allen, and Rik Sarkar. 2021. Multi-Scale attributed node embedding. *Journal of Complex Networks* 9, 2 (05 2021).
- [38] Oleksandr Shchur, Maximilian Mumme, Aleksandar Bojchevski, and Stephan Günnemann. 2018. Pitfalls of graph neural network evaluation. *arXiv preprint arXiv:1811.05868* (2018).
- [39] Daohan Su, Bowen Fan, Zhi Zhang, Haoyan Fu, and Zhida Qin. 2024. DCL: Diversified Graph Recommendation With Contrastive Learning. *IEEE Transactions on Computational Social Systems* (2024).
- [40] Henan Sun, Xunkai Li, Zhengyu Wu, Daohan Su, Rong-Hua Li, and Guoren Wang. 2023. Breaking the Entanglement of Homophily and Heterophily in Semi-supervised Node Classification. *arXiv preprint arXiv:2312.04111* (2023).
- [41] Yifei Sun, Haoran Deng, Yang Yang, Chunping Wang, Jiarong Xu, Renhong Huang, Linfeng Cao, Yang Wang, and Lei Chen. 2022. Beyond Homophily: Structure-aware Path Aggregation Graph Neural Network. In *IJCAI*. 2233–2240.
- [42] Qiaoyu Tan, Xin Zhang, Ninghao Liu, Daochen Zha, Li Li, Rui Chen, Soo-Hyun Choi, and Xia Hu. 2023. Bring your own view: Graph neural networks for link prediction with personalized subgraph selection. In *Proceedings of the ACM International Conference on Web Search and Data Mining, WSDM*.
- [43] Veronika Thost and Jie Chen. 2021. Directed acyclic graph neural networks. *arXiv preprint arXiv:2101.07965* (2021).
- [44] Zekun Tong, Yuxuan Liang, Changsheng Sun, Xinke Li, David Rosenblum, and Andrew Lim. 2020. Digraph inception convolutional networks. *Advances in Neural Information Processing Systems, NeurIPS* (2020).
- [45] Zekun Tong, Yuxuan Liang, Changsheng Sun, David S Rosenblum, and Andrew Lim. 2020. Directed graph convolutional network. *arXiv preprint arXiv:2004.13970* (2020).

- [46] Petar Veličković, Guillem Cucurull, Arantxa Casanova, Adriana Romero, Pietro Lio, and Yoshua Bengio. 2018. Graph attention networks. In *International Conference on Learning Representations, ICLR*.
- [47] Hongwei Wang and Jure Leskovec. 2020. Unifying graph convolutional neural networks and label propagation. *arXiv preprint arXiv:2002.06755* (2020).
- [48] Kuansan Wang, Zhihong Shen, Chiyuan Huang, Chieh-Han Wu, Yuxiao Dong, and Anshul Kanakia. 2020. Microsoft academic graph: When experts are not enough. *Quantitative Science Studies* 1, 1 (2020), 396–413.
- [49] Xiyuan Wang and Muhan Zhang. 2022. How Powerful are Spectral Graph Neural Networks. In *International Conference on Machine Learning, ICML*.
- [50] Felix Wu, Amauri Souza, Tianyi Zhang, Christopher Fifty, Tao Yu, and Kilian Weinberger. 2019. Simplifying graph convolutional networks. In *International Conference on Machine Learning, ICML*.
- [51] Chenxuan Xie, Jiajun Zhou, Shengbo Gong, Jiacheng Wan, Jiaxu Qian, Shanqing Yu, Qi Xuan, and Xiaoniu Yang. 2023. PathMLP: Smooth Path Towards High-order Homophily. *arXiv preprint arXiv:2306.13532* (2023).
- [52] Keyulu Xu, Chengtao Li, Yonglong Tian, Tomohiro Sonobe, Ken-ichi Kawarabayashi, and Stefanie Jegelka. 2018. Representation learning on graphs with jumping knowledge networks. In *International Conference on Machine Learning, ICML*.
- [53] Yujun Yan, Milad Hashemi, Kevin Swersky, Yaoqing Yang, and Danai Koutra. 2022. Two sides of the same coin: Heterophily and oversmoothing in graph convolutional neural networks. *arXiv preprint arXiv:2102.06462* (2022).
- [54] Liangwei Yang, Shengjie Wang, Yunzhe Tao, Jiankai Sun, Xiaolong Liu, Philip S Yu, and Taiqing Wang. 2023. DGRec: Graph Neural Network for Recommendation with Diversified Embedding Generation. In *Proceedings of the ACM International Conference on Web Search and Data Mining, WSDM*.
- [55] Yiding Yang, Xinchao Wang, Mingli Song, Junsong Yuan, and Dacheng Tao. 2021. Spagan: Shortest path graph attention network. *arXiv preprint arXiv:2101.03464* (2021).
- [56] Jie Zhang, Bo Hui, Po-Wei Harn, Min-Te Sun, and Wei-Shinn Ku. 2021. MGC: A complex-valued graph convolutional network for directed graphs. *arXiv e-prints* (2021), arXiv–2110.
- [57] Muhan Zhang and Yixin Chen. 2018. Link prediction based on graph neural networks. *Advances in Neural Information Processing Systems, NeurIPS* (2018).
- [58] Wentao Zhang, Ziqi Yin, Zeang Sheng, Yang Li, Wen Ouyang, Xiaosen Li, Yangyu Tao, Zhi Yang, and Bin Cui. 2022. Graph Attention Multi-Layer Perceptron. *Proceedings of the ACM SIGKDD Conference on Knowledge Discovery and Data Mining, KDD* (2022).
- [59] Xitong Zhang, Yixuan He, Nathan Brugnone, Michael Perlmutter, and Matthew Hirn. 2021. Magnet: A neural network for directed graphs. *Advances in Neural Information Processing Systems, NeurIPS* (2021).
- [60] Xin Zheng, Yixin Liu, Shirui Pan, Miao Zhang, Di Jin, and Philip S Yu. 2022. Graph neural networks for graphs with heterophily: A survey. *arXiv preprint arXiv:2202.07082* (2022).
- [61] Honglu Zhou, Advith Chegu, Samuel S Sohn, Zuohui Fu, Gerard De Melo, and Mubbasir Kapadia. 2022. D-HYPR: Harnessing Neighborhood Modeling and Asymmetry Preservation for Digraph Representation Learning. *Proceedings of the ACM International Conference on Information and Knowledge Management, CIKM* (2022).
- [62] J. Zhu, Y. Yan, L. Zhao, M. Heimann, L. Akoglu, and D. Koutra. 2020. Beyond Homophily in Graph Neural Networks: Current Limitations and Effective Designs. *Advances in Neural Information Processing Systems, NeurIPS* (2020).

A OUTLINE

- A.1 Model implementations in Empirical Study.
- A.2 Datasets Description.
- A.3 Baselines Description.
- A.4 Hyperparameter Settings.
- A.5 Experimental Environment.
- A.6 DiRW Performance in Link Prediction.
- A.7 Sensitivity Analysis.
- A.8 Comparison of DiRW with Other PathGNNs.
- A.9 PathGNN and Graph Attention.

A.1 Model implementations in Empirical Study

Inspired by the concepts of node homophily [31] and edge homophily [62], which are pivotal in understanding the homophily of graphs, we introduce a refined definition of the node homophily ratio for each node:

$$H(u) = \frac{|\{v \in \mathcal{N}_u | y_u = y_v\}|}{|\mathcal{N}_u|}, \quad (15)$$

where \mathcal{N}_u represents the set of neighbors of node u , and y_u denotes the label of node u . The node homophily ratio $H(u)$ serves as a metric for the homophily of the local neighborhood around node u . A higher value of $H(u)$ indicates stronger homophily, meaning node u is more similar to its neighbors in terms of the given label. In experiment, we select the top 50% most homophilous nodes as homophily nodes, while the remaining nodes as heterophily nodes. When investigating the impact of different walk lengths on the model, we fixed the number of walks at 15. Similarly, we fixed the walk length at 4 when exploring the effect of walk numbers.

We utilize the undirected SRW as our sampling strategy. Specifically, each node randomly selects a neighbor from its in-neighbors and out-neighbors as the next target. For each node in the graph, we specify the same number of walks N_{walk} and the same walk length L_{walk} . Once each walk sequence is collected, we concatenate the features of every node in the sequence. Suppose the walk sequence is $\{v_1, v_2, \dots, v_{L_{\text{walk}}}\}$, where v_j represents the j -th node in the walk sequence. For each walk sequence, we concatenate the node features to obtain the path feature vector:

$$\mathbf{h}_{\text{path}} = \text{concat}(\mathbf{h}_{v_1}, \mathbf{h}_{v_2}, \dots, \mathbf{h}_{v_{L_{\text{walk}}}}),$$

where \mathbf{h}_{v_j} denotes the feature vector of node v_j . We then pass this path feature vector through a MLP to obtain the path embedding:

$$\mathbf{z}_{\text{path}} = \text{MLP}(\mathbf{h}_{\text{path}}).$$

For each node, we average the embeddings of its different paths to obtain the node embedding. Let the set of path embeddings for node v be $\{\mathbf{z}_{\text{path}}^{(1)}, \mathbf{z}_{\text{path}}^{(2)}, \dots, \mathbf{z}_{\text{path}}^{(N_{\text{walk}})}\}$. The embedding for node v is:

$$\mathbf{z}_v = \frac{1}{N_{\text{walk}}} \sum_{i=1}^{N_{\text{walk}}} \mathbf{z}_{\text{path}}^{(i)}.$$

Finally, we pass the node embedding \mathbf{z}_v through another MLP for the node classification task:

$$\hat{y}_v = \text{MLP}(\mathbf{z}_v).$$

By leveraging this approach, we effectively utilize path information to enhance node representations, achieving better performance in node classification tasks.

A.2 Datasets Description

We evaluate the performance of DiRW under 9 benchmark datasets, covering both homophilous and heterophilous graphs. We have documented the detailed information of these datasets in the Tab. 4. Below, we introduce the descriptions of these benchmark datasets.

CoraML and **CiteSeer** [5] are two academic citation networks, where individual academic papers are represented as nodes, connected by edges that signify citations made between these papers. Each node is characterized by a binary word vector that encapsulates its textual content, while the class labels correspond to the subject areas to which the papers pertain.

WikiCS [30] is a dataset derived from Wikipedia. It comprises nodes that represent articles within the computer science domain, with edges established based on the hyperlinks that connect these articles. The dataset is organized into 10 distinct classes, each representing a different subfield of computer science. The features are generated from the text content of the respective articles by averaging pre-trained GloVe word embeddings [32], yielding a 300-dimensional vector for each node.

Amazon-Computers [38] is a co-purchase network from Amazon that encapsulates consumer behavior through a graph structure. In this graph, nodes correspond to computer products, and edges denote the instances where products are frequently bought together by customers. The features for each product are derived from the text of product reviews, represented as bag-of-words vectors that capture the essence of customer feedback.

Ogbn-arxiv [14] is a citation network dataset indexed by the MAG [48], which is characterized by the word embeddings found within the titles and abstracts of academic papers. The word embeddings are generated through the application of the skip-gram model, which is for learning vector representations of words.

Ogbn-products [14] is a co-purchasing network where nodes represent products and edges represent two products are frequently bought together. Node features are generated by extracting bag-of-words features from the product descriptions.

Chameleon [37] is a network derived from English Wikipedia, where nodes represent articles and edges indicate mutual backlinks between them. Each node is characterized by a feature set that reflects the presence of specific nouns.

Actor [31] is an actor co-occurrence network where each node symbolizes an actor and the edges indicate instances where actors are mentioned together on Wikipedia pages. The node features in this network are constructed as bag-of-words vectors, which are created by extracting keywords from the Wikipedia pages dedicated to each actor. These features are then sorted into five different categories, each corresponding to the specific terms present on an actor's Wikipedia page.

Rating [34] is a dataset that originates from the Amazon product co-purchasing network metadata found within the SNAP [20]. In this network, nodes correspond to different products, and edges are established between items that are commonly purchased in conjunction with one another. The primary task is to forecast the average rating awarded by reviewers, which is divided into five distinct classes. The node features are formulated from the mean FastText embeddings [10] of the words present in the product descriptions, providing a textual representation of each product.

Table 4: The statistician of the experimental datasets.

Characteristics	Datasets	#Nodes	#Edges	#Features	#Node Classes	#Train/Val/Test	#Description
Directed-Homophily	CoraML	2,995	8,416	2,879	7	140/500/2,355	citation network
	CiteSeer	3,312	4,591	3,703	6	120/500/2,692	citation network
	WikiCS	11,701	290,519	300	10	580/1,769/5,847	weblink network
	Amazon-Computers	13,752	287,209	767	10	200/300/12,881	co-purchase network
	ogbn-arxiv	169,343	2,315,598	128	40	91k/30k/48k	citation network
UnDirected-Homophily	ogbn-products	2,449,029	61,859,140	100	47	196k/49k/2204k	co-purchase network
Directed-Heterophily	Chameleon	890	13,584	2,325	5	48%/32%/20%	wiki-page network
	Actor	7,600	26,659	932	5	48%/32%/20%	actor network
	Rating	24,492	93,050	300	5	50%/25%/25%	rating network

A.3 Baselines Description

Our experiment leverages diverse GNNs as comparative benchmarks, which can be categorized as follows: (i) traditional undirected approaches: GCN [18], GAT [46]; (ii) directed spatial methods: DGCN [45], NSTE [19], DIMPA [13], Dir-GNN [36], ADPA [40]; (iii) directed spectral methods: DiGCN [44] and its variant DiGCNapp [59], MGC [56], LightDiC [22]; (iiii) PathGNNs: RAW-GNN [17] and PathNet [41]. To minimize randomness and ensure fair comparisons, we repeated each experiment 10 times to obtain unbiased performances. Moreover, we transform the digraph to undirected graph and feed it into undirected GNNs. The main features of each baseline model are as follows:

GCN [18]: GCN operates on the principle of a localized first-order spectral graph convolution, which serves as an approximation. It is designed to scale efficiently with the number of edges in the graph. The model processes information through hidden layers that synthesize the local neighborhood structure and individual node features, thereby learning representations that are pertinent to the graph’s topology and node attributes.

GAT [46]: GAT employs attention mechanisms to dynamically assess the significance of neighboring nodes during the aggregation of information. This approach allows for the flexible assignment of varying influence to different nodes within a neighborhood, without the need for predefined knowledge of the graph’s structure.

DGCN [45]: DGCN pioneers a novel message-passing scheme that takes into account both the first and second nearest neighbors’ proximity. This approach results in the development of aggregators that are tailored to differentiate between incoming and outgoing edges, utilizing two distinct sets of parameters that are learned through the training process.

DiGCN [44]: Recognizing the intrinsic relationship between the graph Laplacian and the steady-state distributions of PageRank, DiGCN introduces a theoretical advancement that adapts personalized PageRank to formulate a genuinely symmetric representation of the directed graph Laplacian. Additionally, DiGCN leverages the closeness of both first and second-order neighbors to augment the model’s receptive field.

DiGCNapp [44]: This variant of DiGCN incorporates an efficient approximation for personalized PageRank, streamlined by the absence of inception blocks. It represents a generalized form of GCN that is grounded in the directed graph Laplacian, offering a more nuanced approach to graph convolution for directed networks.

DIMPA [13]: In the DIMPA model, the source and target nodes are distinctly represented. It gathers neighborhood information across multiple hops within each layer to expand the model’s receptive field. Furthermore, DIMPA employs a weighted averaging mechanism for the aggregated multi-hop neighborhood data, which allows it to effectively encapsulate the local network structure.

NSTE [19]: NSTE draws inspiration from the 1-WL graph isomorphism test, utilizing two distinct sets of weights to encode the source and target nodes independently. Subsequently, the model refines the weights used for information aggregation through a parameterized feature propagation process.

Dir-GNN [36]: The Dir-GNN framework is specifically crafted to excel in heterophilous scenarios. It effectively manages the directionality of edges through distinct aggregation processes for incoming and outgoing edges. This approach has been shown to rival the expressiveness of the directed Weisfeiler-Lehman test.

ADPA [40]: ADPA is distinguished by its adaptive exploration of appropriate neighborhood operators of directed k -order for propagation without the need for edge weights. It also incorporates a two-tiered system of node-adaptive attention mechanisms, which are designed to refine and optimize the representation of nodes within the graph. This adaptive methodology allows ADPA to dynamically select the most suitable operators for the given graph structure, leading to enhanced node representation capabilities.

MagNet [59]: MagNet employs the mathematical framework of complex numbers to capture the nuances of directed information flow. It introduces a novel spectral approach to GNNs for digraphs, leveraging the concept of a complex Hermitian matrix termed the magnetic Laplacian. To further enhance predictive accuracy, MagNet incorporates additional parameters that independently merge the real and imaginary components of the filter signals.

MGC [56]: MGC introduces the magnetic Laplacian, a discrete operator that incorporates a magnetic field effect. It also employs a truncated form of the PageRank algorithm, referred to as Linear-Rank, to construct filters tailored for both homogeneous and heterogeneous graphs, with a low-pass and high-pass filter, respectively.

LightDiC [22]: LightDiC is an innovative and scalable adaptation of digraph convolution that is founded on the magnetic Laplacian. It performs all topological computations during an offline pre-processing phase, which showcases its scalability. It allows for the downstream tasks to be trained in an independent manner, without the computational burden with recursive processes.

Table 5: Model performance (%) in link direction prediction. The best result is bold. The second result is underlined.

Models	CoraML	CiteSeer	WikiCS	Amazon Computers	Chameleon	Actor	Rating	Arxiv
GCN	83.63±0.74	74.29±0.73	72.97±0.23	92.42±0.14	87.98±0.48	58.37±1.34	50.16±0.74	82.24±0.12
GAT	81.28±3.40	79.33±2.24	70.18±9.71	67.35±0.85	85.80±1.83	54.13±0.42	50.84±0.88	76.55±4.46
DGCN	89.47±0.25	85.09±0.29	87.02±0.08	95.67±0.13	91.38±0.58	82.58±0.66	78.96±0.10	OOT
DiGCN	88.15±0.57	87.99±1.77	85.38±0.19	96.45±0.09	89.84±0.61	82.77±0.44	80.92±0.05	92.71±0.04
DiGCNapp	84.96±0.23	82.50±0.51	83.41±0.10	95.72±0.07	91.54±1.25	81.60±0.25	78.92±0.06	91.71±0.01
NSTE	90.10±0.59	87.86±0.60	87.69±0.15	95.49±0.56	91.28±0.69	79.74±0.20	80.29±0.39	92.31±0.07
DIMPA	<u>90.48±0.33</u>	86.83±0.50	82.54±0.15	95.65±0.16	89.68±0.69	82.33±0.24	83.06±0.06	93.56±0.12
MagNet	89.25±0.34	85.13±0.60	89.07±0.10	96.73±0.07	90.64±1.18	83.69±0.39	82.75±0.18	93.91±0.04
MGC	89.97±0.64	81.79±1.63	86.66±0.17	86.86±0.46	89.15±0.97	67.84±0.37	72.39±0.17	87.65±4.27
LightDiC	88.87±0.46	87.99±0.46	88.77±0.06	95.30±0.05	90.27±0.36	82.39±0.35	81.59±0.07	92.73±0.01
Dir-GNN	88.95±0.45	86.34±0.99	88.87±0.05	<u>96.93±0.03</u>	<u>91.97±0.63</u>	85.89±0.17	<u>85.01±0.05</u>	<u>94.73±0.05</u>
ADPA	90.28±0.78	<u>88.57±0.68</u>	<u>88.85±0.14</u>	96.66±0.06	89.52±0.83	84.88±0.34	82.69±0.24	93.81±0.04
RAW-GNN	89.92±1.21	87.01±1.04	83.48±0.8	94.93±0.18	89.95±1.21	85.34±0.46	73.26±0.43	OOM
DiRW	91.05±0.57	88.96±1.38	88.79±0.49	97.15±0.24	92.19±1.17	<u>85.56±0.39</u>	85.49±0.34	95.27±0.08

RAW-GNN [17]: RAW-GNN leverages the Node2Vec algorithm to emulate both breadth-first search (BFS) and depth-first search (DFS) traversal techniques. This dual-simulation approach enables the model to encapsulate a comprehensive spectrum of information within the graph, including both the tendencies of nodes to connect with similar and dissimilar neighbors.

PathNet [41]: PathNet is distinguished by its use of a maximal entropy-based random walk strategy. By optimizing for maximal entropy, PathNet ensures a diverse and comprehensive exploration of the graph’s topology, leading to more robust and informative node representations.

A.4 Hyperparameter Settings

The hyperparameters in the baseline GNNs are set following the original paper if available. Otherwise, we perform a hyperparameter search via the Optuna [3]. In DiRW, we perform a grid search for the minimum walking length ranging from 2 to 6, and for the minimum walk number ranging from 2 to 10. Furthermore, we fine-tune the walk direction coefficient q within the interval $[0.5, 1]$.

A.5 Experimental Environment

Our experiments are conducted on the machine with Intel(R) Xeon(R) Platinum 8468V, and NVIDIA H800 PCIe and CUDA 12.2. The operating system is Ubuntu 20.04.6. As for the software, we use Python 3.8 and Pytorch 2.2.1 for implementation.

A.6 DiRW Performance in Link Prediction

In addition to the node classification task, we have conducted a thorough evaluation of DiRW’s performance in the link direction prediction task, with the results presented in Tab. 5. We directly leverage the node embeddings obtained from Eq. (13) and concatenate them to form edge embeddings, with Eq. (14) obviated. This concatenated vector serves as a comprehensive representation of the edges, capturing the characteristics between connected nodes.

The experimental outcomes provide compelling evidence that DiRW excels not only in categorizing nodes but also in predicting the direction of edges, outperforming the leading Dir-GNN by an average of 0.82%. The efficacy of DiRW in link prediction is a testament to its ability to capture the subtleties of graph structure and the nuanced relationships between nodes. This capability stems from the model’s sophisticated path sampling strategies and its attention-based aggregation mechanism, which together allow for a deep understanding of the digraph’s topology and node features.

It is important to note that traditional undirected GNNs have exhibited subpar performance in this task. The primary reason for this deficit lies in the task’s requirement for precise capture of the directional information of edges between nodes, a nuance that conventional undirected methodologies fail to address adequately. In contrast, DiRW’s design explicitly accounts for edge directionality, providing it with a distinct advantage in tasks where the direction of relationships is pivotal. This comparative analysis underscores the importance of adopting models that can accommodate the directed nature of graphs, thereby offering a more accurate representation of the underlying structure and relationships within the data.

A.7 Sensitivity Analysis

To systematically evaluate the influence of hyperparameters on the experimental outcomes, we performed an in-depth analysis focusing on two pivotal parameters: the minimum walk length l_{min} and the minimum walk number n_{min} . The findings of these experiments are depicted in Fig. 7, where all other parameters were kept constant to isolate the effects of l_{min} and n_{min} .

Our analysis reveals a notable trend of improvement in node classification performance as the n_{min} increases. However, it is important to note that the increase in walk numbers, while beneficial for performance, cannot be pursued indefinitely due to the concomitant escalation in time and space complexity, which poses practical limitations. Regarding the minimal walk length, the impact on node classification performance is less straightforward.

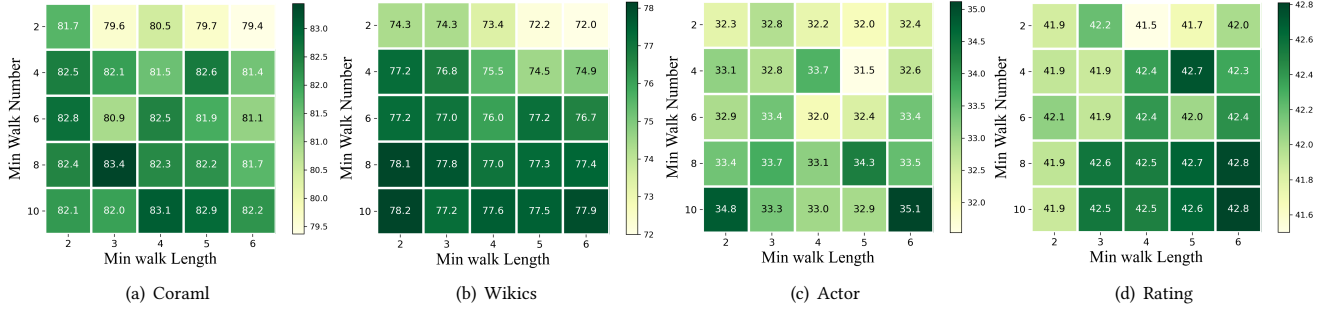


Figure 7: Sensitivity analysis of test accuracy to minimal walk length l_{min} and minimal walk number n_{min} .

There is no definitive pattern of improvement or decline in node classification performance as l_{min} is incremented. Interestingly, our results show that in homophilous digraphs, such as coraml and wikis, shorter walk lengths are more conducive to achieving better performance. In contrast, in heterophilous digraphs like Actor and Amazon-Rating, longer walk lengths are associated with superior performance. This dichotomy is in line with our prior discussions regarding the presence of high-order homophily in heterophilous graphs, which suggests that longer walks are essential for capturing the intricate relationships within these complex digraph structures.

A.8 Comparison of DiRW with Other PathGNNs

Substantial researches acknowledge the capability of path information in distilling the complex structural and homophilous patterns in graphs, thereby enhancing the characterization of node attributes in scenarios marked by heterophily. **GeniePath** [25] proposes an adaptive path layer which consists of two complementary functions designed for breadth and depth exploration. The breadth exploration learns the importance of different one-hop neighborhoods, while the depth exploration captures signals from neighbors of different hops away. **SPAGAN** [55] exploits the shortest path to account for the influence of a sequence of nodes between the center node and its higher-order neighbors. It also conducts path-based attention to obtain a more effective aggregation. **PathNet** [41] designs a maximal entropy-based path sampler to sample paths containing homophilous and structural context. It also introduces a structure-aware RNN to preserve order and distance information, learning the semantic contexts of neighborhoods. **RAWGNN** [17] utilizes Node2Vec [11] to simulate breadth first search and depth first search to capture homophily and heterophily information in graphs, respectively. It also introduces a new path-based aggregator based on RNN. **PathMLP** [51] observes high-order homophily embedded in heterophilous graphs and proposes a light-weight model based on MLP. It designs a similarity-based path sampling strategy to capture paths with high-order homophily for originating nodes.

Despite recent advancements, their walk strategies are tailored for undirected graphs and lack generalizability. Our empirical study in Fig. 1(a) and 1(b) have revealed that naive random walk leads to severe walk interruption problems, which indicates that the majority of walk sequences fail to gather extensive information. To address this challenge, DiRW designs a direction-aware walk strategy to identify potential relationships between the current node and its generalized neighbors through walk sequences. Furthermore, the complex relationships inherent in directed topology pose

unique challenges to the naive random walks, necessitating further investigations to develop fine-grained walk rules. The empirical study in Fig. 2(a) and 2(b) demonstrates that the one-size-fits-all sampling approaches overlook the distinct contexts of nodes within complex topology. To solve this problem, DiRW fine-tunes the walk numbers and walk lengths on a node-adaptive level, providing a rich information source for representing the current node.

It is noteworthy that our proposed homophily entropy is fundamentally different from the maximal entropy random walk (MERW) mentioned in PathNet [41]. The MERW makes use of the maximum entropy rate from information theory in [8], adjusting the walk probabilities to be proportional to the eigenvector centrality. On the other hand, the homophily entropy is designed to inform the walk length instead of guiding the walk probabilities. Furthermore, conceptually, the entropy in MERW depends on the transition probabilities of each node, which are solely determined by the graph’s topological structure. In contrast, the probability distribution used in homophily entropy is based on the features of nodes within a walk sequence, enabling it to measure the quality of the sequence.

A.9 PathGNN and Graph Attention

PathGNNs and graph attention mechanisms are two innovative approaches in graph representation learning, each with its unique methodology for capturing the nuances of graph-structured data.

Graph attention techniques focus on the local structure of graphs to allocate weights among nodes [6]. The process typically unfolds in several distinct steps: (1) Computing node similarities. (2) Yielding attention weights. (3) Aggregating features with weights. The whole process effectively propagates and updates the node features in a manner that reflects their relative importance.

Similarly, PathGNNs systematically sample paths to capture the relationships between nodes. The operation of PathGNNs can be broken down into the following steps: (1) Sampling according to meticulously designed walk probabilities. (2) Forming path features by aggregating the node features along paths. (3) Deriving the node representations by integrating distinct path features. Broadly speaking, PathGNNs can be regarded as a lightweight variant of graph attention mechanisms. Unlike traditional attention models that may involve complex learning processes, PathGNNs rely on a more streamlined sampling procedure, which enhances their scalability. By avoiding the computational overhead associated with learning attention weights, PathGNNs offer a more flexible alternative for graph learning, particularly in heterophilous scenarios.